

# Experimental test of the Rosenzweig-Porter model for the transition from Poisson to Gaussian unitary ensemble statistics

Xiaodong Zhang,<sup>1</sup> Weihua Zhang,<sup>1,2</sup> Jiongning Che,<sup>1</sup> and Barbara Dietz<sup>1,2,\*</sup>

<sup>1</sup>Lanzhou Center for Theoretical Physics and the Gansu Provincial Key Laboratory of Theoretical Physics, Lanzhou University, Lanzhou, Gansu 730000, China

<sup>2</sup>Center for Theoretical Physics of Complex Systems, Institute for Basic Science (IBS), Daejeon 34126, Korea

(Dated: May 23, 2023)

We report on an experimental investigation of the transition of a quantum system with integrable classical dynamics to one with violated time-reversal ( $\mathcal{T}$ ) invariance and chaotic classical counterpart. High-precision experiments are performed with a flat superconducting microwave resonator with circular shape in which  $\mathcal{T}$  invariance and a chaotic dynamics are induced by magnetizing a ferrite disk placed at its center. We determine a complete sequence of  $\simeq 1000$  eigenfrequencies and verify analytical predictions for the spectral properties of the Rosenzweig-Porter (RP) model which, currently, is under intensive study in the context of many-body quantum chaos as it exhibits ergodic, fractal and localized phases. Furthermore, we introduce based on this RP model and the Heidelberg approach a random-matrix model for the scattering ( $S$ ) matrix of the corresponding open quantum system and show that it perfectly reproduces the fluctuation properties of the measured  $S$  matrix of the microwave resonator.

*Introduction.*— In the past four decades, random matrix theory (RMT) [1] experienced outstanding success in the field of quantum chaos, of which the objective is to identify quantum signatures of classical chaos in the properties of quantum systems. Originally, RMT was introduced by Wigner to describe properties of the eigenstates of complex many-body quantum systems. He was the first to propose that there is a connection between their spectral properties and those of random matrices [2–5]. This proposition was taken up in Refs. [6–8] and led to the formulation of the Bohigas-Giannoni-Schmit (BGS) conjecture which states that the spectral properties of all quantum systems, that belong to either the orthogonal, unitary or symplectic universality class and whose classical analogues are chaotic, agree with those of random matrices from the Gaussian orthogonal ensemble (GOE), the Gaussian unitary ensemble (GUE), or the Gaussian symplectic ensemble (GSE), respectively. On the other hand, according to the Berry-Tabor (BT) conjecture [9], the fluctuation properties in the eigenvalue sequences of typical integrable systems exhibit Poissonian statistics. The BGS conjecture was confirmed theoretically [10, 11] and experimentally, e.g., with flat, cylindrical microwave resonators [12–16]. Below the cutoff frequency  $f^{cut} = 7.5$  GHz of the first transverse-electric mode the associated Helmholtz equation is scalar, that is the electric field strength is parallel to the resonator axis and obeys Dirichlet boundary conditions (BCs) along the side wall. Accordingly, there the Helmholtz equation is mathematically identical to the Schrödinger equation of a quantum billiard (QB) of corresponding shape with these BCs and the cavity is referred to as microwave billiard. For generic  $\mathcal{T}$ -invariant systems with chaotic classical counterpart, that

are well described by the GOE [11], complete sequences of up to 5000 eigenfrequencies [17–19] were obtained in high-precision experiments at liquid-helium temperature  $T_{\text{LHe}} = 4$  K with niobium and lead-coated microwave resonators which become superconducting at  $T_c = 9.2$  K and  $T_c = 7.2$  K, respectively. The BGS conjecture also applies to quantum systems with chaotic classical dynamics and partially violated  $\mathcal{T}$  invariance [20–25], that are described by a RMT model interpolating between the GOE and the GUE for complete  $\mathcal{T}$ -invariance violation. They were investigated experimentally in [26–29] and in microwave billiards [30–36]. In addition, the fluctuation properties of the scattering ( $S$ ) matrix of open quantum systems with partially violated  $\mathcal{T}$  invariance where analyzed and exact analytical results were derived based on the Heidelberg approach for quantum-chaotic scattering [37–39]. Here,  $\mathcal{T}$ -invariance violation was induced by inserting a ferrite into the resonator and magnetizing it with an external magnetic field  $B$ . Because of the Meissner-Ochsenfeld effect [40] this is not possible at superconducting conditions with lead-coated cavities [18], since lead is a superconductor of type I [41]. To avoid the expulsion of the external magnetic field, the cavity used in [36] was made from niobium, a type II [42] superconductor for  $153 \text{ mT} \leq B \leq 268 \text{ mT}$ .

In recent years the Rosenzweig-Porter (RP) model [43–54] has come to the fore in the context of many-body quantum chaos and localization since it undergoes on variation of a parameter  $\alpha$  a transition from localized states in the integrable limit via a non-ergodic phase which is characterized by multifractal states to an ergodic phase, where the spectral properties approach those of either the GOE or the GUE, depending on whether  $\mathcal{T}$ -invariance is preserved or not. Here we focus on the latter case,

\* bdietzp@gmail.com

$$\hat{H}^{RP}(\alpha) = \hat{H}_0 + \alpha \hat{H}^{GUE}, \quad (1)$$

where  $\hat{H}_0$  is diagonal with Poissonian distributed entries and  $\hat{H}^{GUE}$  is drawn from the GUE [55]. It interpolates between Poisson for  $\alpha = 0$  and GUE for  $\alpha \rightarrow \infty$ , however, the spectral properties of  $\hat{H}^{RP}(\alpha)$  already coincide with GUE for  $\lambda = \alpha/\langle\rho\rangle \simeq 1$ , where  $\lambda$  gives  $\alpha$  in units of the average level spacing  $D = 1/\langle\rho\rangle$ .

The objective of the Letter is to experimentally investigate the transition from Poisson to GUE, to verify analytical results for the spectral properties of the RP model, and to gain insight into the properties of the corresponding open scattering system. The  $S$ -matrix properties are compared to those for the transition from GOE to GUE and to a RMT model which we introduce for the  $S$  matrix based on the Heidelberg approach. The microwave resonators have the shapes of billiards with integrable dynamics. Ferrites are inserted into them in such a way, that integrability is not destroyed. Magnetization with an external field  $B$  induces  $\mathcal{T}$ -invariance and also chaoticity, as will be shown [56].

*Experiments at room temperature.*— We, first, investi-

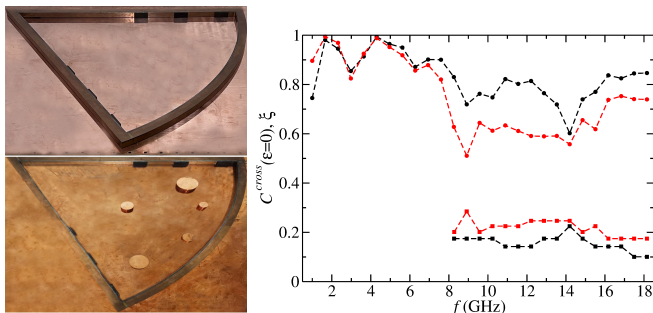


FIG. 1. Left: Photograph of the sector shaped microwave cavity with the top plate removed (top) and with 5 copper disks of varying radius and height 20 mm (bottom). All parts are made from copper. The size of the top and bottom plates are  $1260 \times 860 \times 5 \text{ mm}^3$ . The frame has the shape of a  $60^\circ$  circle sector with radius  $R = 800 \text{ mm}$  and height 20 mm corresponding to a cutoff frequency 7.5 GHz of the first transverse-electric mode. To induce partial  $\mathcal{T}$ -invariance violation, three flat rectangular ferrite pieces (black rectangles) of length 50 mm, width 5 mm and height 20 mm were attached symmetrically to both straight parts of the frame at a distance 425 mm, 575 mm, and 725 mm from the apex and magnetized with an external magnetic field of strength 169 mT. The top and bottom plate and frame were squeezed together tightly with screw clamps. Furthermore, a rectangular frame of the same size as the plates and the same height as the frame, and the top and bottom plates were firmly screwed together. Both frames contained grooves that were filled with a tin-lead alloy to improve the electrical contact. Right: Cross-correlation coefficients of the cavity without (black dots) and with circular disks (red dots) determined in 1 GHz windows. The corresponding values for  $\xi$  are plotted as black and red squares, respectively.

gated the properties of the  $S$  matrix associated with the measurement process of the resonance spectra of a microwave cavity to confirm that the wave dynamics undergoes a transition from Poisson to GUE when inducing  $\mathcal{T}$ -

invariance violation by magnetizing ferrites inserted into it. The measurements were done with the large-scale microwave cavity with the shape of a  $60^\circ$  circle sector used in Ref. [57] and shown in the left upper part of Fig. 1. Six thin ferrite strips made of 18F6 with a saturation magnetization  $M_s = 180 \text{ mT}$  were attached symmetrically to the straight side walls of the circle sector, to ensure integrability of the wave dynamics for zero external magnetic field [15, 58–62]. We checked experimentally for frequencies below  $f^{cut} = 7.5 \text{ GHz}$  that the spectral properties of the microwave billiard with no disks [63, 64] and the one containing five disks as illustrated in the left lower part of Fig. 1 agree with those of a QB whose shape generates an integrable and chaotic dynamics [65–67], respectively, as clearly visible in Fig. A1 of the appendix. Note, that at the walls of the ferrite strips the electric-field strengths obeys mixed Dirichlet-Neumann BCs, however, as demonstrated in Refs. [63, 64] and verified experimentally, the spectral properties of such QBs comply with those of quantum systems with an integrable classical dynamics.

The eigenfrequencies of the cavity correspond to the positions of the resonances in its reflection and transmission spectra,  $|S_{aa}(f)|$  and  $|S_{ab}(f)|$ , with  $S_{ab}(f)$  denoting the matrix elements of the  $S$  matrix. They were measured by attaching antennas  $a, b$  at two of five possible ports distributed over the billiard area and connecting them to a Keysight N5227A Vector Network Analyzer (VNA) via SUCOFLEX126EA/11PC35/1PC35 coaxial cables. It couples microwaves into the resonator via one antenna and receives them at the same or the other one, respectively, and determines the relative amplitude and phase of the output and input signal. To achieve partial  $\mathcal{T}$ -invariance violation we magnetized the ferrite pieces with an external magnetic field  $B = 169 \text{ mT}$  generated with NdFeB magnets that were placed above and below the cavity [30, 32, 68, 69]. Due to absorption of the ferrites, which is especially high for  $B \neq 0$ , Ohmic losses in the walls which leads to overlapping resonances and the integrability of the wave dynamics for  $B = 0 \text{ mT}$  implying resonance clustering, it is not possible to obtain complete sequences of eigenvalues for the normal-conducting resonator. Therefore, we investigated fluctuation properties of the  $S$  matrix instead. Since we are only interested in properties of the  $S$  matrix, we do not need to restrict to the range below  $f^{cut}$ .

We demonstrated in [57], that the fluctuation properties of the  $S$  matrix of the cavity with no ferrites and no or up to three disks, whose spectral properties follow Poisson and intermediate statistics [70], respectively, clearly deviate from those of chaotic scattering systems. We performed RMT simulations based on the scattering formalism for quantum-chaotic scattering [71] in order to analyze the results for the cavity with five disks. The  $S$ -matrix elements of the RMT model,

$$S_{ba}(f) = \delta_{ba} - 2\pi i [\hat{W}^\dagger (f\mathbb{1} - \hat{H} + i\pi\hat{W}\hat{W}^\dagger)^{-1} \hat{W}]_{ba}, \quad (2)$$

depend on a coupling matrix  $\hat{W}$  which accounts for the interaction between the internal states of the Hamiltonian  $\hat{H}$  and the open channels, which comprise the antenna channels and fictitious ones that account for Ohmic losses quantified in terms of a parameter  $\tau_{abs}$ . Furthermore, we replace  $\hat{H}$  by  $\hat{H}(\xi) = \hat{H}^{(S)} + i\xi \frac{\pi}{\sqrt{N}} \hat{H}^{(A)}$ , which models the transition from GOE to GUE [21, 72, 73], and thus, according to the BGS conjecture, the universal spectral properties of the cavity with the strength of partial  $\mathcal{T}$ -invariance determined by the parameter  $\xi$ . Furthermore,  $\hat{H}^{(S)}$  is a real-symmetric random matrix from the GOE and  $\hat{H}^{(A)}$  is real-antisymmetric with Gaussian distributed elements with mean-value zero. For more information we refer the reader to the appendix.

The transmission coefficients associated with the antennas,  $T_c = 1 - |S_{cc}|^2$  with  $c = a, b$ ,  $\xi$  and  $\tau_{abs}$  are the input parameters of the RMT model where they are assumed to be frequency-independent. Accordingly, we analyzed the fluctuation properties of the measured  $S$  matrix in 1 GHz windows [38]. To determine the strength  $\xi$  of  $\mathcal{T}$ -invariance violation we proceeded as in [38, 39, 74] and compared the experimental cross-correlation coefficients  $C_{ab}^{cross}(\epsilon = 0)$  with  $\epsilon$  denoting the microwave frequency in units of the mean resonance spacing, shown in the right part of Fig. 2 as red dots, to exact analytical results for  $C^{cross}(0; \xi, T_a, T_b, \tau_{abs})$ , yielding the values of  $\xi$  shown as red squares in the right part of Fig. 2. For  $\xi = 0$   $\mathcal{T}$  invariance is preserved or, equivalently, the principle of reciprocity  $S_{ab}(f) = S_{ba}(f)$  holds and  $C_{ab}^{cross}(0) = 1$ , whereas fully violated  $\mathcal{T}$  invariance yields  $C_{ab}^{cross}(0) = 0$ . To determine  $\tau_{abs}$  we compared the experimental two-point correlation function  $C_{ab}(\epsilon)$  to exact analytical results for  $C_{ab}(\epsilon; \xi, T_a, T_b, \tau_{abs})$  [38]. Above about 8 GHz  $\mathcal{T}$  invariance is clearly violated.

In Fig. 2 we compare the two-point correlation functions (red dots) and amplitude distributions (red histograms) for different frequency ranges to RMT predictions (turquoise). We observe, that with increasing frequency the results for the cavity with no disks (black dots and black histograms) approach those curves, implying that there a transition from Poisson to GUE takes place. Thus, magnetization of the ferrite pads induces  $\mathcal{T}$ -invariance violation and chaoticity in the dynamics. The orange histograms show the amplitude distributions of the  $S$ -matrix elements Eq. (2) with  $\hat{H}$  replaced by the RP Hamiltonian Eq. (1). We determined the strength of  $\mathcal{T}$ -invariance violation by comparing the experimentally determined  $C_{ab}^{cross}(\epsilon = 0)$ , shown as black dots in the right part of Fig. 1 to the analytical result for the transition from GOE to GUE yielding for the  $\xi$  the values shown as black squares in the right part of Fig. 1. Yet, we found out that the model underestimates its value. Actually, best agreement is found when choosing for  $\lambda = \alpha/D$  the values of  $\xi$  obtained based on the RMT model for the GOE-GUE transitions, given in the caption of Fig. 2.

*Experiments at superconducting conditions.*— We, furthermore, performed experiments at superconducting conditions with a circular microwave billiard contain-

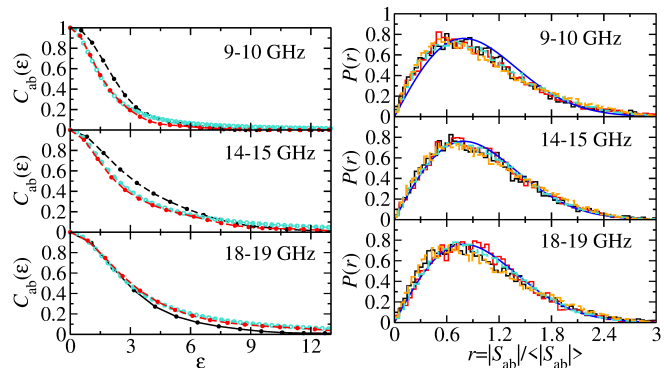


FIG. 2. Two-point correlation functions (left) and distributions of the amplitudes (right) of the  $S$ -matrix for  $a \neq b$  in the frequency ranges indicated in the panels. Here,  $T_a = 0.60, T_b = 0.68, \tau_{abs} = 1.6, \xi = 0.28$  for  $f \in [9, 10]$  GHz,  $T_a = 0.80, T_b = 0.87, \tau_{abs} = 2.5, \xi = 0.2$  for  $f \in [14, 15]$  GHz and  $T_a = 0.86, T_b = 0.89, \tau_{abs} = 3.75, \xi = 0.185$  for  $f \in [18, 19]$  GHz. Shown are the results for the cavity without (black) and with (red) disks and the analytical (left) and Monte-Carlo RMT results (right) for Eq. (1) with  $\hat{H}$  replaced by  $\hat{H}(\xi)$  (turquoise) and  $\hat{H}^{RP}(\alpha)$  (orange); see main text. The blue solid curve shows the RMT prediction for the Ericson regime of strongly overlapping resonances.

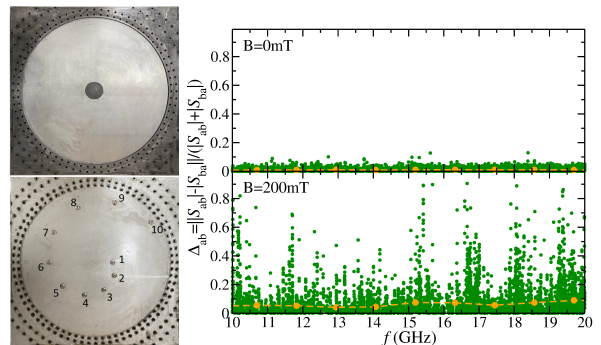


FIG. 3. Left: Photograph of the 5 mm thick lead-coated brass plate with a circular hole on top of a niobium plate (top) and the niobium lid (bottom) of the microwave billiard. The radius of the circle is  $R = 250$  mm and the cavity height equals  $h = 5$  mm corresponding to a cutoff frequency  $f^{cut} = 30$  GHz. A ferrite disk made of 19G3 with saturation magnetization  $M_s = 195$  mT with radius 30 mm and same height as the cavity is placed at its center. In total 10 ports were fixed to the lid. The three plates are screwed together tightly through holes along the cavity boundary and circles visible in the photographs, and tin-lead is filled into grooves that were milled into the top and bottom surfaces of the middle plate along the circle boundary. Right: Relative size of violation of the principle of detailed balance for  $B = 0$  mT and  $B = 200$  mT, respectively. The orange dots connected by dashed line show the average values in a sliding 1 GHz windows.

ing a ferrite disk at the center, shown in Fig. 3, to investigate spectral properties of quantum systems that undergo a transition from integrable classical dynamics with preserved  $\mathcal{T}$  invariance to a chaotic one with

complete  $\mathcal{T}$ -invariance violation. To induce  $\mathcal{T}$ -invariance violation the ferrite is magnetized with a static magnetic field of strength  $B = 200$  mT that is generated with two external NdFeB magnets, fixed above and below the cavity [36]. To achieve a high quality factor of  $Q \gtrsim 5 \cdot 10^4$ , the cavity was cooled down to about 5 K in a cryogenic chamber constructed by ULVAC Cryogenics in Kyoto, Japan. We thereby could determine a complete sequence of 1014 eigenfrequencies in the frequency range 10-20 GHz, using the resonance spectra measured between the antennas for all port combinations. The measurements were performed for  $B = 200$  mT and for  $B = 0$  mT also with a metallic circle disk instead of the ferrite disk, which corresponds to an integrable ring-shaped QB. The effect of magnetization is that the resonances are slightly shifted and part of them are missing (see Fig. A2 of the appendix). In the right part of Fig. 3 we show  $\Delta_{ab} = [||S_{ab}| - |S_{ba}||]/[|S_{ab}| + |S_{ba}|]$ , which gives a measure for the violation of detailed balance,  $|S_{ab}| = |S_{ba}|$ , and thus for the strength of  $\mathcal{T}$ -invariance violation. For  $B = 0$  mT is fulfilled up to experimental accuracy, whereas for  $B = 200$  mT it is clearly violated. In Fig. A3 of the appendix we show examples for the intensity distributions of the non-vanishing electric- and magnetic-field components in the cavity with magnetized ferrite. The patterns exhibit clear distortions with respect to those for the case  $B = 0$  mT where, e.g., the electric-field distributions resemble the wave functions of the ring-shaped QB. As demonstrated in the following, these lead to clear deviations from Poisson statistics, that can not be explained by a RP model for the transition from Poisson to GOE.

For the analysis of the spectral properties we unfolded the eigenfrequencies to mean spacing one, by replacing them by the spectral average of the integrated resonance density  $\langle N(f) \rangle$ ,  $\epsilon_i = \langle N(f_i) \rangle$ , which for the metallic disk is given by Weyl's formula,  $\langle N(f) \rangle = \frac{A\pi}{c^2} f^2 - \frac{\mathcal{L}}{2c} f + N_0$ , with  $A$  and  $\mathcal{L}$  denoting the area and perimeter of the billiard, respectively, and provides a good approximation for the ferrite disk for  $B = 0$  mT. For  $B \neq 0$  mT we determined  $\langle N(f) \rangle$  by fitting a quadratic polynomial to the experimentally determined number of eigenfrequencies  $f_i \in [0, f]$ ,  $N(f)$ . We analyzed the spectral properties in terms of the nearest-neighbor spacing distribution  $P(s)$ , the cumulative nearest-neighbor spacing distribution  $I(s)$ , the number variance  $\Sigma^2(L) = \langle (N(L) - \langle N(L) \rangle)^2 \rangle$  with  $\langle N(L) \rangle = L$ , and the power spectrum  $s(\tau) = \left\langle \left| \frac{1}{\sqrt{n}} \sum_{q=0}^{n-1} \delta_q \exp(-2\pi i \tau q) \right|^2 \right\rangle$  with  $\delta_q = \epsilon_{q+1} - \epsilon_1 - q$  for a complete sequence of  $n$  levels, where  $0 \leq \tau \leq 1$  [75, 76]. Furthermore, we considered the distribution of the ratios [77, 78] of consecutive spacings between next-nearest neighbors,  $r_j = \frac{f_{j+1} - f_j}{f_j - f_{j-1}}$ . They are dimensionless so that no unfolding is needed [77–79]. We compared these measures to analytical ones for the RP model Eq. (1). In [80, 81] a Wigner-surmise like expression was derived for the nearest-neighbor spacing distribution, and in [23–25] approximations for the two-point

cluster function and number variance. For completeness, the results are provided in the appendix Eqs. (A4)-(A7).

In the left part of Fig. A4 of the appendix we show spectral properties for  $B = 0$  mT and a metallic or ferrite disk at the circle center. The curves lie on top of each other and coincide with analytical results for the corresponding ring QB, that is, the agreement with Poisson is as good as expected for  $\approx 1000$  levels. In the right part are exhibited the spectral properties for  $B = 200$  mT in the range  $[0, 20]$  GHz, which also comprises  $\approx 1000$  levels. They agree well with the RP model for  $\lambda = 0.214$ . Furthermore, we compare the length spectra for the microwave billiard with metallic disk at the center, i.e., the ring QB, with those with a ferrite disk and  $B = 0$  mT and  $B = 200$  mT, respectively, to illustrate that periodic orbits of the circular QB are effected which hit the disk.

We also analyzed the spectral properties in frequency intervals of approximately constant  $\Delta_{ab}$  (see Fig. 3). The results are shown together with the analytical curves in Fig. 4. The corresponding values of  $\lambda$  are given in the figure caption. The largest achieved chaoticity and  $\mathcal{T}$ -invariance violation value equals  $\lambda = 0.27$ . Deviations are visible in the long-range correlations beyond a certain value of  $L$ . This may be attributed to the comparatively small number of eigenvalues  $n$  given in the figure caption. Above all, the analytical models provide a good approximation for the spectral properties of the RP Hamiltonian only beyond a certain value of  $\lambda$ . However, we performed Monte-Carlo simulations with  $400 \times 400$  random matrices of the form Eq. (1) and found that the approximation is good for the relevant range of  $\lambda$  values.

*Conclusions.*– We propose an experimental setup consisting of a circular microwave cavity with a magnetized ferrite disk at the center, for the study of the properties of typical quantum systems, whose classical counterpart experiences a transition from integrable with preserved  $\mathcal{T}$ -invariance to chaotic with partially violated  $\mathcal{T}$  variance. Indeed, the fluctuation properties of the  $S$  matrix of the corresponding open system are well described by the Heidelberg approach Eq. (2) with the Hamiltonian replaced by the RP Hamiltonian Eq. (1). Furthermore, the spectral properties agree with those of the eigenvalues of the RP Hamiltonian Eq. (1). We confirmed this by comparing them to Monte-Carlo simulations for random matrices of the form Eq. (1) and verified analytical results derived in [22–25, 81]. The experiments were performed at superconducting conditions with a cavity whose bottom plate and lid are constructed from niobium, a superconductor of type II [42]. This is a crucial prerequisite to render possible the determination of complete sequence of  $\approx 1000$  eigenfrequencies. Thereby, we were able to analyze the spectral properties in various frequency ranges and thus, to observe the gradual transition from Poisson to GUE.

This work was supported by the NSF of China under Grant Nos. 11775100, 12247101 and 11961131009. WZ acknowledges financial support from the China Scholarship Council (No. CSC-202106180044). BD and WZ ac-

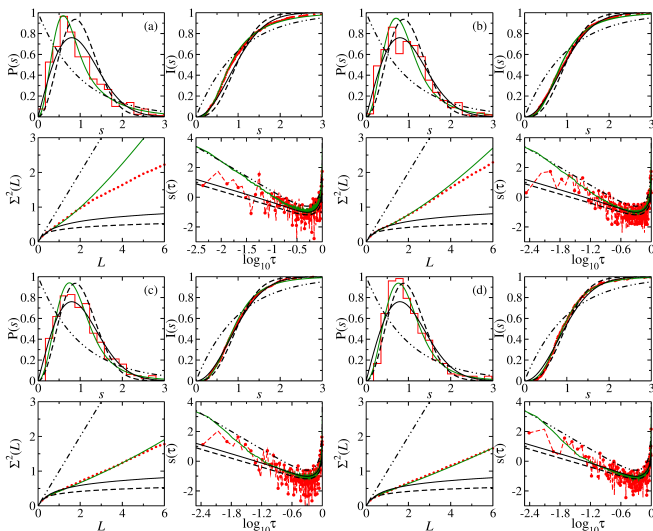


FIG. 4. Spectral properties of the circular microwave billiard with a ferrite disk for  $B = 200$  mT (red histograms and dots). They are compared to the curves deduced from Eqs. (A4)-(A7) of the appendix (green curves) and results for Poisson (black dashed-dot-dot lines), GOE (solid black line) and GUE (dashed black lines) statistics. Shown are the results for (a)  $n = 231$ ,  $f_i \in [10, 13]$  GHz, (b)  $n = 294$ ,  $f_i \in [13, 16]$  GHz, (c)  $n = 232$ ,  $f_i \in [16, 18]$  GHz and (d)  $n = 256$ ,  $f_i \in [18, 20]$  GHz, with  $\lambda = 0.146, 0.203, 0.225, 0.27$ , respectively.

knowledge financial support from the Institute for Basic Science in Korea through the project IBS-R024-D1.

XZ and WZ contributed equally to the work.

### Appendix A: Spectral properties of the sector-shape cavity containing five disks

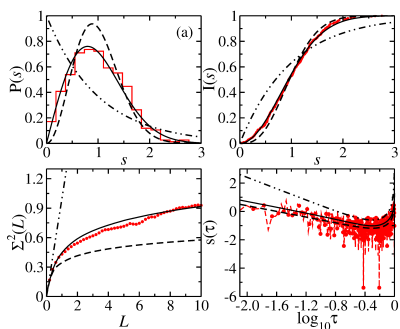


FIG. A5. Nearest-neighbor spacing distribution  $P(s)$ , cumulative nearest-neighbor spacing distribution  $I(s)$ , number variance  $\Sigma^2(L)$  and power spectrum  $s(\tau)$  for the sector-shaped microwave billiard containing five metal disks. They agree well with GOE. The solid, dashed and dashed-dot-dot black lines show the curves for GOE, GUE and Poisson statistics, respectively.

### Appendix B: The scattering formalism for quantum chaotic scattering undergoing a transition from GOE to GUE

Exact analytical results for the fluctuation properties of the  $S$  matrix describing a quantum-chaotic scattering process in the presence of partial  $\mathcal{T}$ -invariance violation were derived based on the scattering matrix approach [71] which was developed in the context of compound nuclear reactions and extended to microwave resonators in [82],

$$S_{ba}(f) = \delta_{ba} - 2\pi i [\hat{W}^\dagger (f \mathbb{1} - \hat{H}^{eff})^{-1} \hat{W}]_{ba}, \quad (\text{A1})$$

where  $a, b$  denote the antenna channels. Here,  $\hat{H}^{eff} = \hat{H} - i\pi \hat{W} \hat{W}^\dagger$  with  $\hat{H} = \hat{H}^{(S)} + i\xi \frac{\pi}{\sqrt{N}} \hat{H}^{(A)}$  modeling the universal spectral properties of the microwave billiard with the magnitude of the partial  $\mathcal{T}$ -invariance determined by the parameter  $\xi$ . Furthermore,  $\hat{H}^{(S)}$  and  $\hat{H}^{(A)}$  denote a real-symmetric and real-antisymmetric random matrix with Gaussian distributed elements  $h_{ij}$  with mean-value zero and variance  $\langle h_{ii}^2 \rangle = 2 \langle h_{i \neq j}^2 \rangle = 1$ , respectively. The matrix elements of  $\hat{W}$  are real, Gaussian distributed with  $W_{a\mu}$  and  $W_{b\mu}$  describing the coupling of the antenna channels to the resonator modes. Furthermore, we introduced  $\Lambda$  fictitious channels that account for the Ohmic losses in the walls of the resonator [38, 39] in terms of a parameter  $\tau_{abs}$ . We ensured that, as assumed in the RMT model, direct transmission between the antennas is negligible, that is, that the frequency-averaged  $S$ -matrix is diagonal [83], implying that  $\sum_{\mu=1}^N W_{e\mu} W_{e'\mu} = N v_e^2 \delta_{ee'}$  [83]. The parameters  $v_e^2$  denote the average strength of the coupling of the resonances to channels  $e$ . For  $e = a, b$  they correspond to the average size of the electric field at the position of the antennas  $a$  and  $b$  and they yield the transmission coefficients  $T_e = 1 - \langle |S_{ee}| \rangle^2$ , which are experimentally accessible [39].

To determine the strength  $\xi$  of  $\mathcal{T}$ -invariance violation we employed the experimental cross-correlation coefficients

$$C_{ab}^{cross}(0) = \text{Re}[\langle S_{ab}^{fl}(f) S_{ba}^{*fl}(f) \rangle] / \sqrt{\langle |S_{ab}^{fl}(f)|^2 \rangle \langle |S_{ba}^{fl}(f)|^2 \rangle} \quad (\text{A2})$$

proceeding as in [38, 39, 74]. Accordingly, we compared them to exact analytical results for  $C_{ab}^{cross}(0; \xi, T_a, T_b, \tau_{abs})$  to determine the strength  $\xi$  of  $\mathcal{T}$ -invariance violation for given values of  $T_a, T_b$  and an approximate value for  $\tau_{abs}$  using that they depend only weakly on small changes of that parameter. For  $\xi = 0$   $\mathcal{T}$  invariance is preserved or, equivalently, the principle of reciprocity  $S_{ab}(f) = S_{ba}(f)$  holds and  $C_{ab}^{cross}(0) = 1$ , whereas fully violated  $\mathcal{T}$  invariance yields  $C_{ab}^{cross}(0) = 0$ . To determine  $\tau_{abs}$  we compared the experimental two-point correlation function  $C_{ab}(\epsilon) = \langle S_{ab}^{fl}(\nu) S_{ab}^{*fl}(\nu + \epsilon) \rangle$  with  $\nu$  and  $\epsilon$  denoting the microwave frequency and frequency-increment in units of the average resonance spacing, to exact analytical results for  $C_{ab}(\epsilon; \xi, T_a, T_b, \tau_{abs})$  [38, 39].

### Appendix C: Analytical results for the spectral properties of quantum systems undergoing a transition from Poisson to GUE

The analytical results were obtained for the Rosenzweig-Porter RMT model consisting of Hermitian matrices of the form

$$\hat{H} = \hat{H}^{Poi} + \alpha H^{GUE} \quad (\text{A1})$$

interpolating between Poisson for  $\alpha = 0$  and GUE for  $\alpha \rightarrow \infty$ . Note, that the spectral properties of  $\hat{H}$  coincide with GUE already for  $\lambda = \alpha \langle \rho \rangle \simeq 1$  with  $\langle \rho \rangle$  denoting the average resonance density. When choosing for the off-diagonal entries of the  $N \times N$ -dimensional  $\hat{H}$  variance unity, it is given by  $\langle \rho \rangle = \sqrt{N}/\pi$ . In [80, 81] a Wigner-surmise like expression was derived for the nearest-neighbor spacing distribution based on the RMT model with  $N = 2$ ,

$$P_{0 \rightarrow 2}(s; \alpha) = C s^2 e^{-D^2 s^2} \int_0^\infty dx e^{-\frac{x^2}{4\alpha^2} - x} \frac{\sinh z}{z}, \quad (\text{A2})$$

$$D(\alpha) = \frac{1}{\sqrt{\pi}} + \frac{1}{2\alpha} e^{\alpha^2} \operatorname{erfc}(\alpha) - \frac{\alpha}{2} \operatorname{Ei}(\alpha^2)$$

$$+ \frac{2\alpha^2}{\sqrt{\pi}} {}_2F_2\left(\frac{1}{2}, 1; \frac{3}{2}, \frac{3}{2}; \alpha^2\right),$$

$$C(\alpha) = \frac{4D^3(\alpha)}{\sqrt{\pi}}, \quad z = \frac{xDs}{\alpha},$$

where  $\operatorname{erfc}$  denotes the complementary error function,  $\operatorname{Ei}$  the exponential integral, and  ${}_2F_2$  the generalized hypergeometric error function [84, 85]. In [23–25] analytical expressions were derived for the number variance,

$$\Sigma_{0 \rightarrow 2}^2(L; \lambda) = \Sigma_{GUE}^2(L) + \frac{2L}{\pi} \arctan\left(\frac{L}{\pi\lambda^2}\right) \quad (\text{A3})$$

$$- \left(\lambda^2 + \frac{1}{2\pi^2}\right) \ln\left(1 + \frac{L^2}{\pi^2\lambda^4}\right) + \frac{1}{2\pi^2} \frac{L^2\pi^2\lambda^4 - L^4}{(L^2 + \pi^2\lambda^4)^2},$$

and the two-point cluster function

$$Y_{2;0 \rightarrow 2}(r; \lambda) = \frac{1}{2(\pi r)^2} \left[1 - e^{-\frac{r^2}{\lambda^2}} \cos(2\pi r)\right] - \frac{1}{\pi} \frac{\pi\lambda^2}{r^2 + \pi^2\lambda^4}, \quad (\text{A4})$$

which yields the result for the power spectrum

$$s_{0 \rightarrow 2}(\tau) = \frac{1}{4\pi^2} \left[ \frac{K_{0 \rightarrow 2}(\tau) - 1}{\tau^2} + \frac{K_{0 \rightarrow 2}(1 - \tau) - 1}{(1 - \tau)^2} \right]$$

$$+ \frac{1}{4 \sin^2(\pi\tilde{\tau})} - \frac{1}{12}. \quad (\text{A5})$$

Here,  $1 - K(\tau) = b_{0 \rightarrow 2}(\tau) = \int_{-\infty}^{\infty} Y_{2;0 \rightarrow 2}(r) e^{-ir\tau} dr$ .

These results provide good approximations for sufficiently large  $\lambda$ . Deviations from the theoretical curves are expected beyond a certain value of  $L$  [24, 25]. We performed Monte-Carlo simulations based on the RMT model Eq. (??) to confirm its applicability in the parameter range relevant for the experiments.

### Appendix D: Additional figures concerning the experiments with the circular microwave billiard

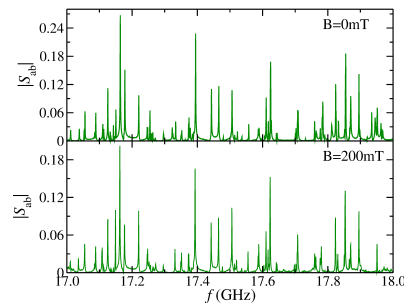


FIG. A6. Part of the transmission spectrum of the circular microwave billiard measured at  $\approx 5$  K for external magnetic field  $B = 0$  mT and  $B = 200$  mT.

In Fig. A6 we compare measured transmission spectra of the cavity with a ferrite disk at the center for  $B = 0$  mT and  $B = 200$  mT. In the latter one resonances are missing or shifted with respect to those for  $B = 0$  mT. This effect of  $\mathcal{T}$ -invariance violation leads to the deviation of the spectral properties from Poisson. Actually, we conclude from the results that magnetizing the ferrite leads to a potential at the circle center that destroys integrability and induces  $\mathcal{T}$ -invariance violation. We show in Fig. A7 examples of computed distributions of the electric field which, for  $B = 0$  mT, below  $f^{cut} = 30$  GHz corresponds to the wave functions of the ring QB, and distributions of the nonzero magnetic-field components of the microwaves. The external magnetic field leads to a distortion of those of the corresponding ring-shaped microwave billiard. The effect is strong enough to induce clear deviations of the spectral properties from Poisson statistics.

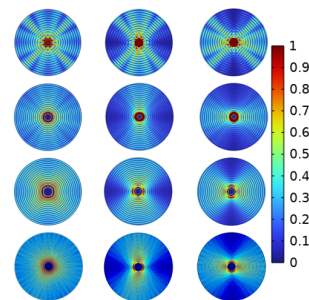


FIG. A7. Intensity distribution of the electric field component of the electromagnetic waves along the cavity axis, that is in  $z$  direction,  $|E_z|$ , (first column) and the magnetic field components in  $x$  and  $y$  direction (second and third column, respectively), for, from top to bottom,  $f = 8.8943, 10xi., 9249, 11.2167, 19.0182$  GHz.

In the left part of Fig. A8 we show spectral properties for  $B = 0$  mT and a metallic or ferrite disk at the circle center. The curves lie on top of each other and coincide with analytical results for the corresponding ring

QB, that is, the agreement with Poisson is as good as expected for  $\approx 1000$  levels. In the right part are exhibited the spectral properties for  $B = 200$  mT in the range  $[0, 20]$  GHz, which also comprises  $\approx 1000$  levels. They agree well with the RP model for  $\lambda = \alpha D = 0.214$ .

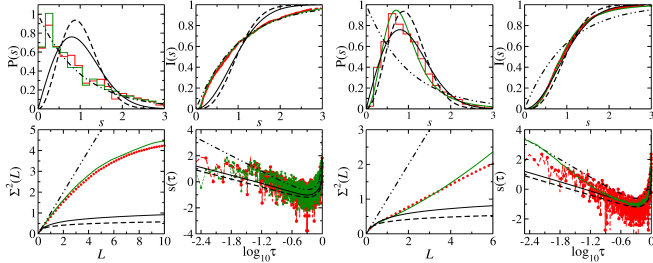


FIG. A8. Left: Spectral properties of the circular microwave billiard with a metallic disk (green histogram and squares) and a ferrite disk (red histogram and dots) at the center for 1014 eigenfrequencies in the frequency range  $[10, 20]$  GHz. They are compared to the results for Poisson (black dashed-dot-dot lines), GOE (solid black line) and GUE (dashed black lines) statistics. Right: Same as left part for  $B = 200$  mT. Here, the green lines show the curves deduced from Eqs. (A4)-(A7) for  $\lambda = 0.214$ .

We also analyzed length spectra of the three microwave billiard systems. A length spectrum is given by the modulus of the Fourier transform of the fluctuating part of the spectral density from wave number to length and has the property that it exhibits peaks at the lengths of the periodic orbits of the corresponding classical system. The left part of Fig. A9 shows the length spectra for the case  $B = 0$  mT and a metallic scatterer, respectively, a ferrite disk at the center of the circle. Both length spectra exhibit peaks at the lengths of orbits of the corresponding ring QB. Some peaks are either weakened or suppressed for the ferrite disk. This is attributed to the differing boundary conditions, implying that in the classical limit there is no specular (hard-wall) reflection at the inner circle. For  $B = 200$  mT some peaks are suppressed or disappear, implying that the corresponding periodic orbits do not exist anymore. These are orbits, that hit the disk at the center of the circular billiard, marked by yellow arrows. Furthermore, we show some periodic orbits. The corresponding peaks are marked by green arrows.

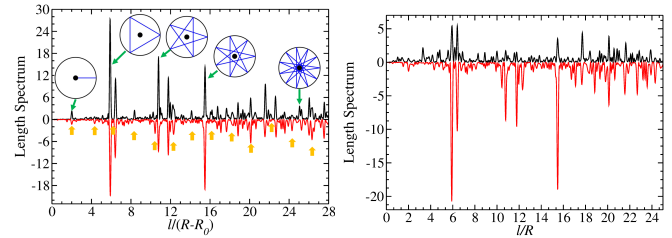


FIG. A9. Left: Length spectra of the circular microwave billiard with a ferrite disk (red solid line) and a metallic disk (black solid line). Right: Length spectra of the circular microwave billiard with a ferrite and  $B = 200$  mT (black solid line) and  $B = 0$  mT (red solid line).

- [1] M. L. Mehta, *Random Matrices* (Elsevier, Amsterdam, 2004).
- [2] C. E. Porter, *Statistical Theories of Spectra: Fluctuations* (Academic, New York, 1965).
- [3] T. A. Brody, J. Flores, J. B. French, P. A. Mello, A. Pandey, and S. S. M. Wong, Random-matrix physics: spectrum and strength fluctuations, *Rev. Mod. Phys.* **53**, 385 (1981).
- [4] T. Guhr and H. A. Weidenmüller, Coexistence of collectivity and chaos in nuclei, *Ann. Phys.* **193**, 472 (1989).
- [5] H. Weidenmüller and G. Mitchell, Random matrices and chaos in nuclear physics: Nuclear structure, *Rev. Mod. Phys.* **81**, 539 (2009).
- [6] M. Berry, *Structural stability in physics* (Pergamon Press, Berlin, 1979).
- [7] G. Casati, F. Valz-Gris, and I. Guarnieri, On the connection between quantization of nonintegrable systems and statistical theory of spectra, *Lett. Nuovo Cimento* **28**, 279 (1980).
- [8] O. Bohigas, M. J. Giannoni, and C. Schmit, Characterization of chaotic quantum spectra and universality of level fluctuation laws, *Phys. Rev. Lett.* **52**, 1 (1984).
- [9] M. V. Berry, Regular and irregular semiclassical wavefunctions, *J. Phys. A* **10**, 2083 (1977).
- [10] M. Giannoni, A. Voros, and J. Zinn-Justin, eds., *Chaos and Quantum Physics* (Elsevier, Amsterdam, 1989).
- [11] F. Haake, S. Gnutzmann, and M. Kuś, *Quantum Signatures of Chaos* (Springer-Verlag, Heidelberg, 2018).
- [12] S. Sridhar, Experimental observation of scarred eigenfunctions of chaotic microwave cavities, *Phys. Rev. Lett.* **67**, 785 (1991).
- [13] J. Stein and H.-J. Stöckmann, Experimental determination of billiard wave functions, *Phys. Rev. Lett.* **68**, 2867

- (1992).
- [14] H.-D. Gräf, H. L. Harney, H. Lengeler, C. H. Lewenkopf, C. Rangacharyulu, A. Richter, P. Schardt, and H. A. Weidenmüller, Distribution of eigenmodes in a superconducting stadium billiard with chaotic dynamics, *Phys. Rev. Lett.* **69**, 1296 (1992).
- [15] S. Deus, P. M. Koch, and L. Sirko, Statistical properties of the eigenfrequency distribution of three-dimensional microwave cavities, *Phys. Rev. E* **52**, 1146 (1995).
- [16] H.-J. Stöckmann, *Quantum Chaos: An Introduction* (Cambridge University Press, Cambridge, 2000).
- [17] A. Richter, Playing billiards with microwaves - quantum manifestations of classical chaos, in *Emerging Applications of Number Theory*, The IMA Volumes in Mathematics and its Applications, Vol. 109, edited by D. A. Hejhal, J. Friedman, M. C. Gutzwiller, and A. M.

- Odlyzko (Springer, New York, 1999) p. 479.
- [18] B. Dietz and A. Richter, Quantum and wave dynamical chaos in superconducting microwave billiards, *Chaos* **25**, 097601 (2015).
- [19] B. Dietz and A. Richter, From graphene to fullerene: experiments with microwave photonic crystals, *Phys. Scr.* **94**, 014002 (2019).
- [20] O. Bohigas, M.-J. Giannoni, A. M. O. de Almeida, and C. Schmit, Chaotic dynamics and the goe-gue transition, *Nonlinearity* **8**, 203 (1995).
- [21] A. Pandey and P. Shukla, Eigenvalue correlations in the circular ensembles, *J. Phys. A* **24**, 3907 (1991).
- [22] G. Lenz, *Zufallsmatrixtheorie und Nichtgleichgewichtsprozesse der Niveaudynamik*, Ph.D. thesis, Fachbereich Physik der Universität-Gesamthochschule Essen (1992).
- [23] T. Guhr, Transitions toward quantum chaos: With supersymmetry from poisson to gauss, *Ann. Phys.* **250**, 145 (1996).
- [24] H. Kunz and B. Shapiro, Transition from poisson to gaussian unitary statistics: The two-point correlation function, *Phys. Rev. E* **58**, 400 (1998).
- [25] K. M. Frahm, T. Guhr, and A. Müller-Groeling, Between poisson and gue statistics: Role of the breit-wigner width, *Ann. Phys.* **270**, 292 (1998).
- [26] J. B. French, V. K. B. Kota, A. Pandey, and S. Tomsovic, Bound on time-reversal noninvariance in the nuclear hamiltonian, *Phys. Rev. Lett.* **54**, 2313 (1985).
- [27] G. E. Mitchell, A. Richter, and H. A. Weidenmüller, Random matrices and chaos in nuclear physics: Nuclear reactions, *Rev. Mod. Phys.* **82**, 2845 (2010).
- [28] M. Aßmann, J. Thewes, D. Fröhlich, and M. Bayer, Quantum chaos and breaking of all anti-unitary symmetries in Rydberg excitons, *Nature Materials* **15**, 741 (2016).
- [29] Z. Pluhař, H. A. Weidenmüller, J. Zuk, C. Lewenkopf, and F. Wegner, Crossover from orthogonal to unitary symmetry for ballistic electron transport in chaotic microstructures, *Ann. Phys.* **243**, 1 (1995).
- [30] P. So, S. M. Anlage, E. Ott, and R. Oerter, Wave chaos experiments with and without time reversal symmetry: GUE and GOE statistics, *Phys. Rev. Lett.* **74**, 2662 (1995).
- [31] U. Stoffregen, J. Stein, H.-J. Stöckmann, M. Kuś, and F. Haake, Microwave billiards with broken time reversal symmetry, *Phys. Rev. Lett.* **74**, 2666 (1995).
- [32] D. H. Wu, J. S. A. Bridgewater, A. Gokirmak, and S. M. Anlage, Probability amplitude fluctuations in experimental wave chaotic eigenmodes with and without time-reversal symmetry, *Phys. Rev. Lett.* **81**, 2890 (1998).
- [33] O. Hul, S. Bauch, P. Pakoński, N. Savvitsky, K. Życzkowski, and L. Sirko, Experimental simulation of quantum graphs by microwave networks, *Phys. Rev. E* **69**, 056205 (2004).
- [34] M. Białous, V. Yunko, S. Bauch, M. Ławniczak, B. Dietz, and L. Sirko, Power spectrum analysis and missing level statistics of microwave graphs with violated time reversal invariance, *Phys. Rev. Lett.* **117**, 144101 (2016).
- [35] M. Allgaier, S. Gehler, S. Barkhofen, H.-J. Stöckmann, and U. Kuhl, Spectral properties of microwave graphs with local absorption, *Phys. Rev. E* **89**, 022925 (2014).
- [36] B. Dietz, T. Klaus, M. Miski-Oglu, A. Richter, and M. Wunderle, Partial time-reversal invariance violation in a flat, superconducting microwave cavity with the shape of a chaotic Africa billiard, *Phys. Rev. Lett.* **123**, 174101 (2019).
- [37] B. Dietz, T. Friedrich, J. Metz, M. Miski-Oglu, A. Richter, F. Schäfer, and C. A. Stafford, Rabi oscillations at exceptional points in microwave billiards, *Phys. Rev. E* **75**, 027201 (2007).
- [38] B. Dietz, T. Friedrich, H. L. Harney, M. Miski-Oglu, A. Richter, F. Schäfer, J. Verbaarschot, and H. A. Weidenmüller, Induced violation of time-reversal invariance in the regime of weakly overlapping resonances, *Phys. Rev. Lett.* **103**, 064101 (2009).
- [39] B. Dietz, T. Friedrich, H. L. Harney, M. Miski-Oglu, A. Richter, F. Schäfer, and H. A. Weidenmüller, Quantum chaotic scattering in microwave resonators, *Phys. Rev. E* **81**, 036205 (2010).
- [40] W. Meissner and R. Ochsenfeld, Ein neuer Effekt bei Eintritt der Supraleitung, *Die Naturwissenschaften* **21**, 787 (1933).
- [41] H. K. Onnes, *Further experiments with liquid helium. G. On the electrical resistance of pure metals, ect. VI. On the sudden change in the rate at which the resistance of mercury disappears* (Comm. from the Phys. Lab., Leiden, 1911).
- [42] L. V. Shubnikov, V. I. Ehotkevich, Y. D. Shepelev, and Y. N. Riabinin, Magnetic properties of superconducting metals and alloys, *Zh. Eksper. Teor. Fiz.* **7**, 221–237 (1937).
- [43] N. Rosenzweig and C. Porter, "repulsion of energy levels" in complex atomic spectra, *Phys. Rev.* **120**, 1698 (1960).
- [44] V. E. Kravtsov, I. M. Khaymovich, E. Cuevas, and M. Amini, A random matrix model with localization and ergodic transitions, *New J. Phys.* **17**, 122002 (2015).
- [45] D. Facchetti, P. Vivo, and G. Biroli, From non-ergodic eigenvectors to local resolvent statistics and back: A random matrix perspective, *Europhys. Lett.* **115**, 47003 (2016).
- [46] K. Truong and A. Ossipov, Eigenvectors under a generic perturbation: Non-perturbative results from the random matrix approach, *Europhys. Lett.* **116**, 37002 (2016).
- [47] C. Monthus, Multifractality of eigenstates in the delocalized non-ergodic phase of some random matrix models: Wigner-Weisskopf approach, *J. Phys. A: Math. Theor.* **50**, 295101 (2017).
- [48] P. von Soosten and S. Warzel, Non-ergodic delocalization in the Rosenzweig-Porter model, *Lett. Math. Phys.* **109**, 905 (2019).
- [49] M. Pino, J. Tabanera, and P. Serna, From ergodic to non-ergodic chaos in Rosenzweig-Porter model, *J. Phys. A: Math. Theor.* **52**, 475101 (2019).
- [50] G. D. Tomasi, M. Amini, S. Bera, I. M. Khaymovich, and V. E. Kravtsov, Survival probability in Generalized Rosenzweig-Porter random matrix ensemble, *SciPost Phys.* **6**, 014 (2019).
- [51] E. Bogomolny and M. Sieber, Eigenfunction distribution for the Rosenzweig-Porter model, *Phys. Rev. E* **98**, 032139 (2018).
- [52] R. Berkovits, Super-Poissonian behavior of the Rosenzweig-Porter model in the nonergodic extended regime, *Phys. Rev. B* **102**, 165140 (2020).
- [53] I. M. Khaymovich, V. E. Kravtsov, B. L. Altshuler, and L. B. Ioffe, Fragile extended phases in the log-normal Rosenzweig-Porter model, *Phys. Rev. Res.* **2**, 043346 (2020).
- [54] M. A. Skvortsov, M. Amini, and V. E. Kravtsov, Sen-



- sitivity of (multi)fractal eigenstates to a perturbation of the Hamiltonian, *Phys. Rev. B* **106**, 054208 (2022).
- [55] B. Dietz, T. Klaus, M. Miski-Oglu, A. Richter, M. Wunderle, and C. Bouazza, Spectral properties of Dirac billiards at the van Hove singularities, *Phys. Rev. Lett.* **116**, 023901 (2016).
- [56] W. Zhang, X. Zhang, J. Che, and B. Dietz,  $T$  violation and chaotic dynamics induced by magnetized ferrite, *Eur. Phys. J.* (2023), "submitted".
- [57] R. Zhang, W. Zhang, B. Dietz, G. Chai, and L. Huang, Experimental investigation of the fluctuations in non-chaotic scattering in microwave billiards, *Chinese Physics B* **28**, 100502 (2019).
- [58] R. L. Weaver, Spectral statistics in elastodynamics, *J. Acoust. Soc. Am.* **85**, 1005 (1989).
- [59] C. Ellegaard, T. Guhr, K. Lindemann, H. Lorensen, J. Nygård, and M. Oxborrow, Spectral statistics of acoustic resonances in aluminum blocks, *Phys. Rev. Lett.* **75**, 1546 (1995).
- [60] H. Alt, H.-D. Gräf, R. Hofferbert, C. Rangacharyulu, H. Rehfeld, A. Richter, P. Schardt, and A. Wirzba, Chaotic dynamics in a three-dimensional superconducting microwave billiard, *Phys. Rev. E* **54**, 2303 (1996).
- [61] H. Alt, C. Dembowski, H.-D. Gräf, R. Hofferbert, H. Rehfeld, A. Richter, R. Schuhmann, and T. Weiland, Wave dynamical chaos in a superconducting three-dimensional sinai billiard, *Phys. Rev. Lett.* **79**, 1026 (1997).
- [62] C. Dembowski, B. Dietz, H.-D. Gräf, A. Heine, T. Papenbrock, A. Richter, and C. Richter, Experimental test of a trace formula for a chaotic three-dimensional microwave cavity, *Phys. Rev. Lett.* **89**, 064101 (2002).
- [63] M. V. Berry and M. R. Dennis, Boundary-condition-varying circle billiards and gratings: the dirichlet singularity, *J. Phys. A* **41**, 135203 (2008).
- [64] E. Bogomolny, M. R. Dennis, and R. Dubertrand, Near integrable systems, *J. Phys. A: Math. Theor.* **42**, 335102 (2009).
- [65] Y. G. Sinai, Dynamical systems with elastic reflections, *Russ. Math. Surv.* **25**, 137 (1970).
- [66] L. A. Bunimovich, On the ergodic properties of nowhere dispersing billiards, *Commun. Math. Phys.* **65**, 295 (1979).
- [67] M. V. Berry, Regularity and chaos in classical mechanics, illustrated by three deformations of a circular 'billiard', *Eur. J. Phys.* **2**, 91 (1981).
- [68] H. Schanze, E. R. P. Alves, C. H. Lewenkopf, and H.-J. Stöckmann, Transmission fluctuations in chaotic microwave billiards with and without time-reversal symmetry, *Phys. Rev. E* **64**, 065201 (2001).
- [69] B. Dietz, T. Friedrich, H. L. Harney, M. Miski-Oglu, A. Richter, F. Schäfer, and H. A. Weidenmüller, Induced time-reversal symmetry breaking observed in microwave billiards, *Phys. Rev. Lett.* **98**, 074103 (2007).
- [70] E. B. Bogomolny, U. Gerland, and C. Schmit, Models of intermediate spectral statistics, *Phys. Rev. E* **59**, R1315 (1999).
- [71] C. Mahaux and H. A. Weidenmüller, *Shell Model Approach to Nuclear Reactions* (North Holland, Amsterdam, 1969).
- [72] A. Pandey, *Ann. Phys.* **134**, 110 (1981).
- [73] A. Altland, S. Iida, and K. B. Efetov, The crossover between orthogonal and unitary symmetry in small disordered systems: a supersymmetry approach, *Journal of Physics A: Mathematical and General* **26**, 3545 (1993).
- [74] M. Białous, B. Dietz, and L. Sirko, How time-reversal-invariance violation leads to enhanced backscattering with increasing openness of a wave-chaotic system, *Phys. Rev. E* **102**, 042206 (2020).
- [75] A. Relaño, J. M. G. Gómez, R. A. Molina, J. Retamosa, and E. Faleiro, Quantum chaos and  $1/f$  noise, *Phys. Rev. Lett.* **89**, 244102 (2002).
- [76] E. Faleiro, J. M. G. Gómez, R. A. Molina, L. Muñoz, A. Relaño, and J. Retamosa, Theoretical derivation of  $1/f$  noise in quantum chaos, *Phys. Rev. Lett.* **93**, 244101 (2004).
- [77] V. Oganesyan and D. A. Huse, Localization of interacting fermions at high temperature, *Phys. Rev. B* **75**, 155111 (2007).
- [78] Y. Y. Atas, E. Bogomolny, O. Giraud, and G. Roux, Distribution of the ratio of consecutive level spacings in random matrix ensembles, *Phys. Rev. Lett.* **110**, 084101 (2013).
- [79] Y. Atas, E. Bogomolny, O. Giraud, P. Vivo, and E. Vivo, Joint probability densities of level spacing ratios in random matrices, *J. Phys. A* **46**, 355204 (2013).
- [80] V. K. B. Kota and S. Sumedha, Transition curves for the variance of the nearest neighbor spacing distribution for poisson to gaussian orthogonal and unitary ensemble transitions, *Phys. Rev. E* **60**, 3405 (1999).
- [81] S. Schierenberg, F. Bruckmann, and T. Wettig, Wigner surmise for mixed symmetry classes in random matrix theory, *Phys. Rev. E* **85**, 061130 (2012).
- [82] S. Albeverio, F. Haake, P. Kurasov, M. Kuś, and P. Šeba, S-matrix, resonances, and wave functions for transport through billiards with leads, *J. Math. Phys.* **37**, 4888 (1996).
- [83] J. Verbaarschot, H. Weidenmüller, and M. Zirnbauer, Grassmann integration in stochastic quantum physics: The case of compound-nucleus scattering, *Phys. Rep.* **129**, 367 (1985).
- [84] M. Abramowitz and I. A. Stegun, eds., *Handbook of Mathematical Functions with Formulas, Graphs and Mathematical Tables* (Dover, New York, 2013).
- [85] I. S. Gradshteyn and I. M. Ryzhik, eds., *Tables of Integrals, Series and Products* (Elsevier, Amsterdam, 2007).